

# Optimisation and Assessment of the Total Impulse Capability of the T6 Ion Thruster

IEPC-2007-231

*Presented at the 30<sup>th</sup> International Electric Propulsion Conference, Florence, Italy  
September 17-20, 2007*

Mr. N. C. Wallace\* and Dr. Michael Corbett†  
QinetiQ Ltd., Cody Technology Park, Farnborough, Hampshire, GU14 0LX, UK

**Abstract:** The design of the T6 ion thruster grid system is described with particular emphasis on the optimization of the grid system to meet the challenging total impulse requirements of the next generation of scientific (BepiColombo) and commercial (AlphaBus) applications. Grid design and testing was performed under the sponsorship of the European Space Agency (ESA) as part of a Technology Readiness Programme and a Technology Demonstration Activity. As part of these programmes a single set of grids were manufactured and tested on a T6 thruster, accumulating a total impulse of  $\sim 3.6 \times 10^6$  Ns at a constant thrust level of 168 mN. The thruster was tested in the QinetiQ LEEP2 and Alta IV4 vacuum test facilities accumulating a total operating time of 6056 hours. The erosion of the Accel grid was measured six times (at approximately 1000 hr intervals) during the test campaign using a 3 axis coordinate measurement machine. These measurements allowed the evolution of the apertures and downstream face of the grid to be assessed and extrapolated indicating a comfortable positive total impulse margin with respect to the AlphaBus and BepiColombo applications.

## Nomenclature

TRP	=	Technology Readiness Programme
TDA	=	Technology Demonstration Activity
TCF	=	Thrust Correction Factor
ESTEC	=	European Space Technology Centre
Ns	=	Newton seconds (impulse)
mN	=	milli-Newton
IV4	=	6m dia x 9m long cryogenic EP vacuum test facility (Alta, Pisa)
LEEP2	=	4m dia x 10m long cryogenic EP vacuum test facility (QinetiQ, Farnborough)
CNC	=	computer numerically controlled
TAG	=	Thick Accel Grid
CEX	=	charge exchange
CMM	=	Coordinate Measurement Machine

---

\* Electric Propulsion Chief Engineer, Space Department, S&DU, ncwallace@qinetiq.com

† Electric Propulsion Scientist, Space Department, S&DU, mhcorbett@qinetiq.com

## I. Introduction

The T6 ion thruster employs a twin grid configuration with an inner grid, often referred to as the screen grid, and an outer grid referred to as the Accelerator (Accel) grid. It is generally recognized that the principle life limiting mechanism associated with all gridded ion thrusters is the erosion of the Accel grid. This erosion mechanism, which is described in more detail in section II, is unavoidable and common to any gridded ion thruster. The process evolves steadily as the impulse delivered by the thruster is accumulated, to the point where either the mechanical integrity or the electric field imposed by the Accel grid is insufficient to prevent electrons emitted by the external neutraliser cathode from penetrating the Accel grid apertures and entering the thruster, a process referred to as electron back-streaming. In both scenarios the thruster is considered to have reached its end of life condition and therefore determines the total impulse (Ns) capability of the device.

At the outset of the studies into the BepiColombo mission to Mercury and the next generation of European communications spacecraft (AlphaBus) it was apparent that these would demand significantly higher Ns performance capabilities than previous applications. In response to these future requirements the European Space Technology Centre (ESTEC) initiated a Technology Readiness Programme (TRP) and a Technology Demonstration Activity (TDA) aimed at developing and optimizing the T6 grid system and subsequently verifying by test the performance and Ns capability.

The planned endurance test campaign consisted of 2500 hours testing under the TDA and 3000 hours under the TRP. During the course of the test campaign additional hours were also performed resulting in a total of 2887 hours under the TDA and a total of 3169 hours operation accumulated under the TRP. At the end of both test programmes therefore a total of 6056 hours have been accumulated on a single set of grids operating at a constant extracted beam current of 2.47A (175mN electrically calculated). After the thrust correction factor (TCF) is applied the total impulse accumulated on the grids set is  $\sim 3.6 \times 10^6$  Ns. Testing was performed in the QinetiQ LEEP2 vacuum facility with the exception of the final 1200 hours which were performed in the new Alta IV4 test facility.

The endurance test campaign the test was interrupted on 6 occasions at 625hrs, 1826hrs, 2925hrs, 4042hrs, 4840hrs and 6056hrs and the erosion of the Accel grid apertures measured. The measurements, which are described in detail in section III, were made using a coordinate measurement machine and allowed the evolution of the diameter and shape of the apertures on the grid throughout the endurance test to be assessed.

## II. T6 Ion thruster

A photograph of a T6 ion thruster and a thruster operating in the Alta test facility is presented in Fig. II-1. It is of conventional Kaufman configuration, with a direct current (DC) discharge between a hollow cathode and a cylindrical anode used to ionise the propellant gas. A schematic of the thruster is also presented in Fig. II-2.

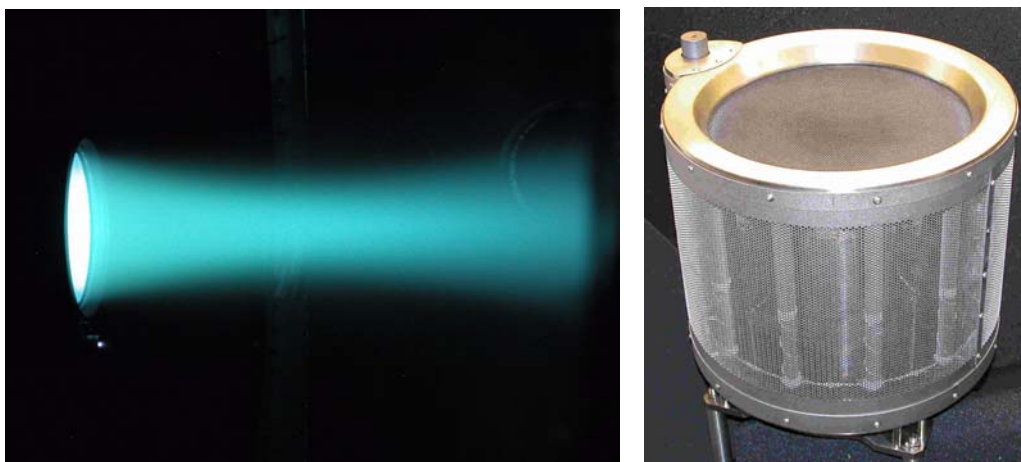
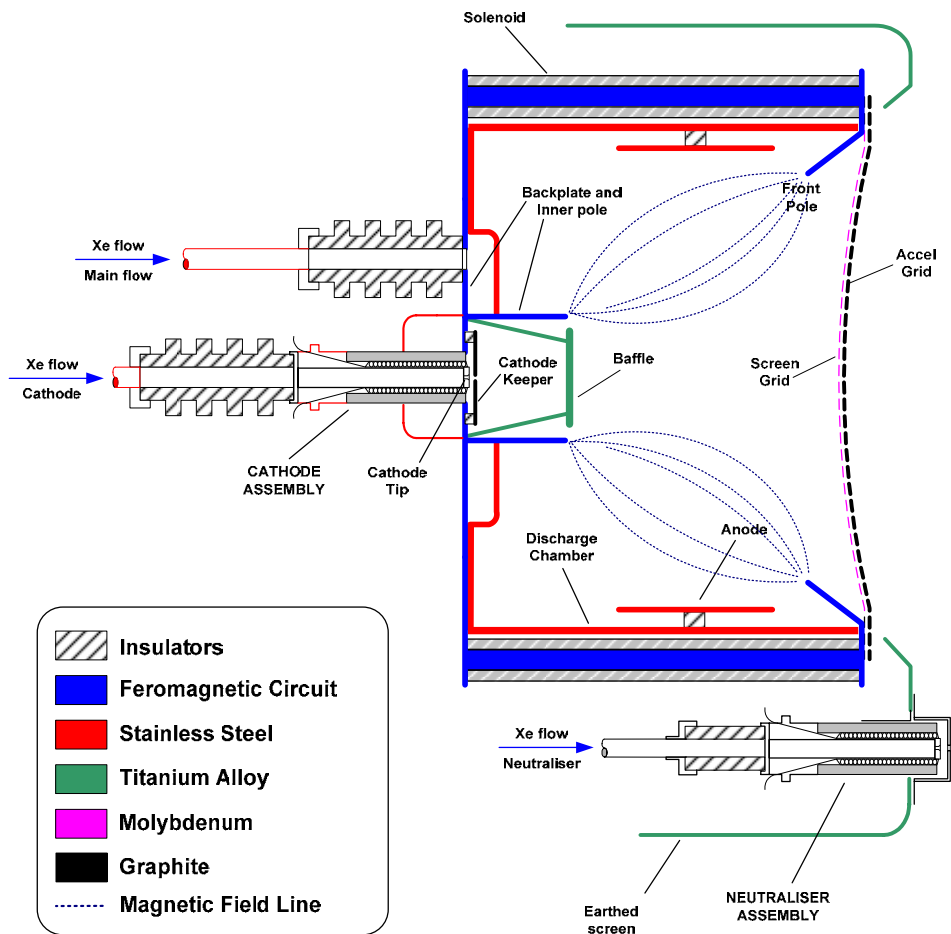


Figure II-1 Photograph of a T6 ion thruster operating in the Alta vacuum test facility



**Figure II-2 T6 ion thruster schematic**

The efficiency of this plasma production process is enhanced by the application of a weak magnetic field within the discharge chamber. This is generated using solenoids which allow the field strength to be tailored to a wide range of discharge conditions allowing the discharge to be optimized and varied across a wide range.

A 22cm diameter grid system, forming the exit to the discharge chamber, extracts and accelerates the ions, to provide the required thrust. The velocity of the ejected ions depends only on the beam potential; whereas the thrust is a function of this and the ion beam current. An external hollow cathode, referred to as the neutraliser, emits the electrons necessary to neutralise the space charge of the emerging ion beam. The flow of propellant through the cathode and neutraliser is fixed regardless of the thrust level. The main propellant flow branch is supplied through the xenon flow controller which adjusts the flowrate to match the desired thrust level.

The discharge chamber is biased at the beam potential and is isolated from the thruster enclosure by high purity alumina ceramic isolators. These isolators are fully shielded to prevent the deposition of any sputter products from either the thruster or ground test facilities, as are all isolators used in the T6, including the grid assembly.

The ion optics system is a concave twin grid arrangement composed of a carbon Accel grid in conjunction with a molybdenum Screen grid, see section A. The grid assembly is carefully designed to maximise the achievable thrust level and total impulse capability whilst minimising ion beam divergence and thrust vector drift. The thruster is constructed using a limited number of freely available and frequently used materials resulting in a relatively low cost and low mass assembly.

### A. T6 Grid system configuration and design

The T6 grid system is comprised of two grids, which are independently mounted to the front magnetic pole piece. The assembly can therefore be treated as a separate mechanical assembly that can be mounted or de-mounted from the rest of the thruster, see Fig. II-3. The grids are spherically dished and are concave with respect to the discharge chamber; i.e. the centre of the grids protrude into the discharge chamber.

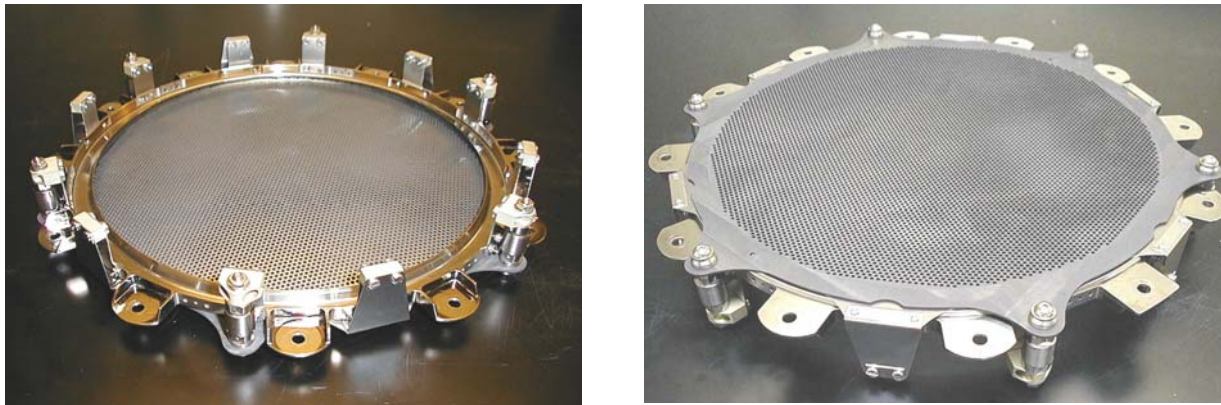


**Figure II-3 Photographs showing upstream and downstream views of the T6 grid assembly**

The inner Screen grid is fabricated from pressed and heat treated molybdenum sheet and the ~7450 apertures are produced by spark erosion. The spark erosion tool consists of 7450 carbon pins ground to a high tolerance on diameter and packed in a hexagonal pattern. Using this tool a screen grid 'blank' can be perforated with all apertures in approximately 3 hours. The Screen grid is mounted to the front pole via flexible mounts that allow for the differential thermal expansion between the front pole and grid.

The outer Accel grid is fabricated from high purity, high density amorphous graphite and is manufactured using standard computer numerically controlled (CNC) machining techniques, including the drilling of the 7450 apertures. The grid is mounted to the front pole via flexible supports and sputter shielded alumina insulators.

The front pole is in turn supported off the top of the solenoid cores and since the assembly mass is relatively small the stiffness of the solenoid cores can be adjusted so that they act as effective mechanical vibration filters; i.e. mechanical inputs to the base of the thruster are not transmitted to the grids. This is a highly useful feature which effectively protects the grids from the severe vibration or shock inputs to the thruster assembly, the effectiveness of which is illustrated by the successful testing of the T6 to the extremely severe vibration and shock levels imposed by the AlphaBus programme.

Any gridded ion thruster exhibits a plasma density profile across the diameter of the discharge chamber and in the case of the T6 thruster there is a naturally higher plasma density on the centerline than at the periphery. As a consequence, if the apertures in the screen grid all had the same diameter the number of ions extracted by the grids would be greater at the centre than at the periphery. The erosion rate of the Accel grid would therefore be greater at the centre and would therefore represent the life limiting point on the grid.

The ion optics of the T6 however is optimized to provide the maximum total impulse. This is achieved by designing the apertures in the screen grid such that the erosion rate on the Accel grid is even across the diameter of the grid, in effect the screen grid aperture diameters are the inverse of the plasma density. The optimization employed on the T6 screen grid, developed as part of the TRP activity is presented in Fig. II-4.

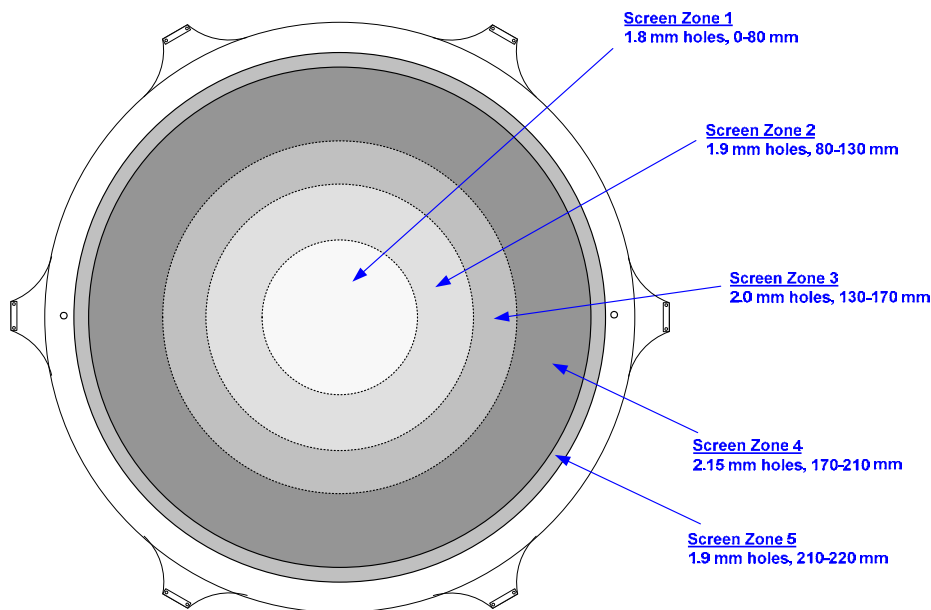


**Figure II-4 Optimisation of the screen grid by varying the aperture diameters**

In addition to optimizing the screen grid the apertures in the Accel grid are made as small as possible and the grid is made as thick as possible, providing as much material as possible for erosion thus maximizing the  $N_s$  capability.

The Thick Accel Grid (TAG) design was developed as part of the TRP activity and has a thickness of 1.2 mm. The apertures, which in the case of the Accel grid are all the same size, are 1.6mm in diameter.

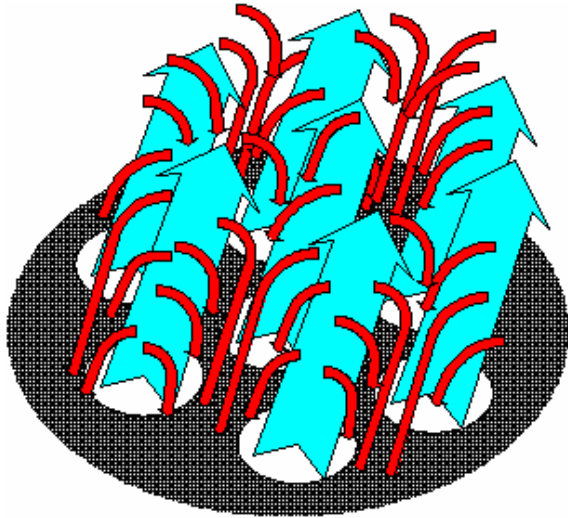
## B. Accel grid erosion mechanism and characteristics

Accel grid erosion, which is unavoidable and common to any gridded ion thruster, is caused by the bombardment of charge exchange (CEX) ions on the surface of the accel grid. CEX ions are created in the inter grid gap or immediately downstream of the grids when a fast moving ion passes sufficiently close to a slow moving neutral escaping through the grids or emitted from the neutraliser. In this condition a ‘charge-exchange’ reaction can occur in which an electron is transferred from the neutral to the ion. The original high energy beam ion continues on the same trajectory as a fast neutral. The newly created CEX ion however does not possess the linear momentum imparted by the focused electric field between the grids and its trajectory is then governed by the electric field at the point where it was produced. A fraction of the CEX ions are therefore accelerated towards the negatively biased Accel grid, bombard the surface causing sputter erosion on impact.

This mechanism cannot be eliminated and occurs at all thrust levels. It can however be minimized by controlling the neutral propellant number density. During operation in space these neutrals can only come from the thruster and neutraliser and therefore the rate at which neutral propellant is lost from the thruster must be minimized. To this end the propellant flow through the neutraliser is minimized and the propellant utilisation efficiency ( $\eta_m$ ) of the discharge chamber, defined as the fraction of propellant usefully employed in the ion beam divided by the total propellant flowed in to the discharge chamber, is maintained at as high a level as possible. This minimizes the CEX ion production rate and the accel grid erosion rate whilst also maximizing the thruster SI.

During ground testing however there is an additional population of neutrals which originate from the facility background pressure because of a limited pumping speed. The erosion of the Accel grid in a ground vacuum facility is therefore higher than in space and represents the design driver in terms of total impulse.

CEX erosion of the Accel grid in a twin grid configuration exhibits two distinct characteristics. The first appears on the downstream face of the Accel grid and is often referred to as ‘pits and grooves’. The schematic presented in Fig II-5 demonstrates how this occurs and Fig. II-6 presents a schematic and photograph of the effects. In Fig. II-5 the **BLUE** arrows represent the individual beamlet ions ejected by single apertures, whilst the **RED** arrows are CEX ions that are streaming towards the thruster. These are produced some distance downstream of the thruster by charge exchange reactions between the facility background gases (mainly neutral propellant atoms) and the ion beam.



The CEX ions are repelled by the beamlets and therefore effectively channeled into regions of lessening charge density, which are situated between the beamlets. In particular points between any three beamlets have less charge than regions between any two. The CEX ions are then accelerated towards the exposed grid web and strike it. The resulting erosion pattern complements the geometric configuration of apertures creating hexagonal erosion patterns as shown below. Regions on the grid with the deepest erosion correspond to minima in the charge density above the face of the grid.

**Figure II-5 Schematic of charge exchange ions being channeled between the beamlets**

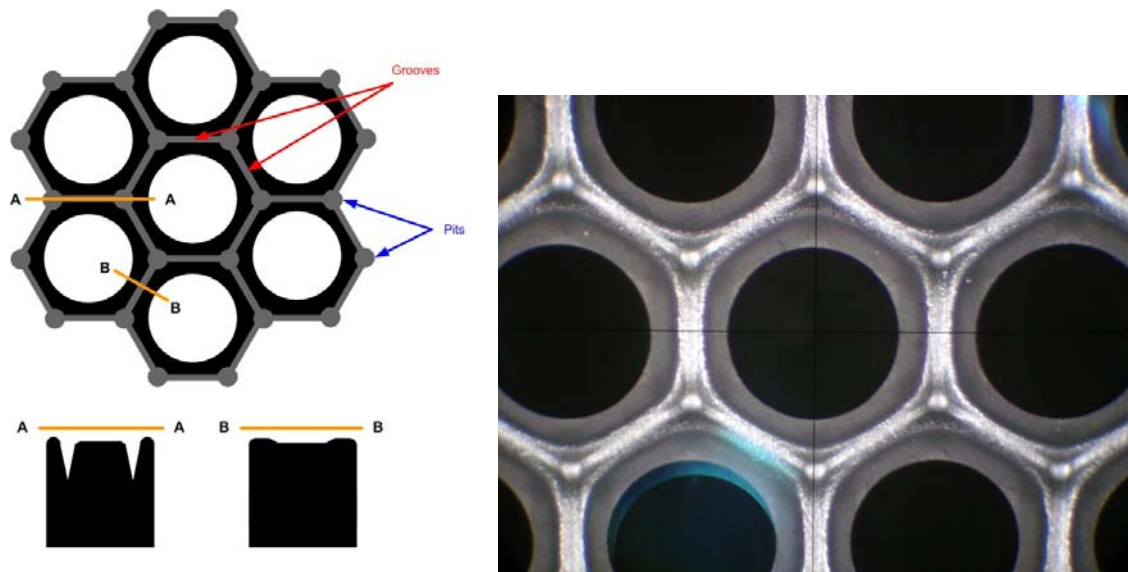


**Figure II-6 Schematic and photograph showing the pit and groove erosion on the downstream face of the Accel grid**

At the same time as the pits and grooves are developing, CEX ions are also eroding the apertures. This results in an increase in the open area of the downstream face of the grid. More erosion occurs at the downstream ends of the apertures than at the upstream region, resulting in the originally cylindrical apertures developing a conical shape, as illustrated in Fig II-7.

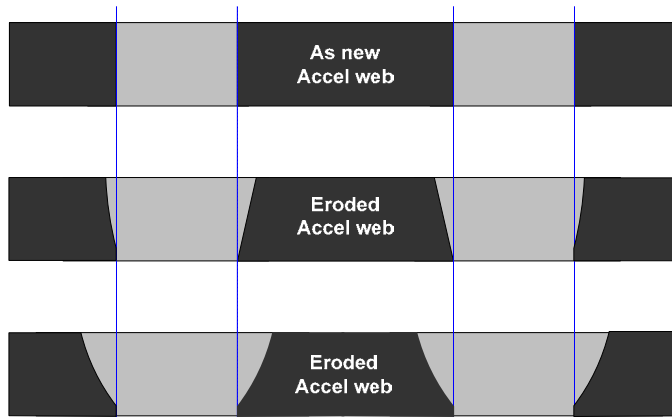


**Figure II-7 Schematic showing the shape of 2 Accel grid apertures at BOL and two stages**

Aperture erosion is the key limiting factor in grid lifetime; i.e. the onset of electron back streaming is made more likely with apertures with larger diameter and thinner cross section.

### III. Accel grid erosion measurement technique and analysis

Aperture measurements were performed using a sub-micron 3-axis coordinate measurement machine (CMM) which senses contact with the grid surface using a ruby tipped stylus. Initially measurements were attempted using a non contact optical technique but this was found to produce inconsistent results between operators. The CMM also allowed the automated measurement of each aperture at different depths as illustrated in Fig. III-1. This also allowed the aperture profile to be determined. Measurements were performed at 0.1 mm, 0.25 mm, 0.4 mm, 0.55 mm, 0.7 mm, 0.85 mm and 1.0 mm depths w.r.t. the downstream surface of the grid.

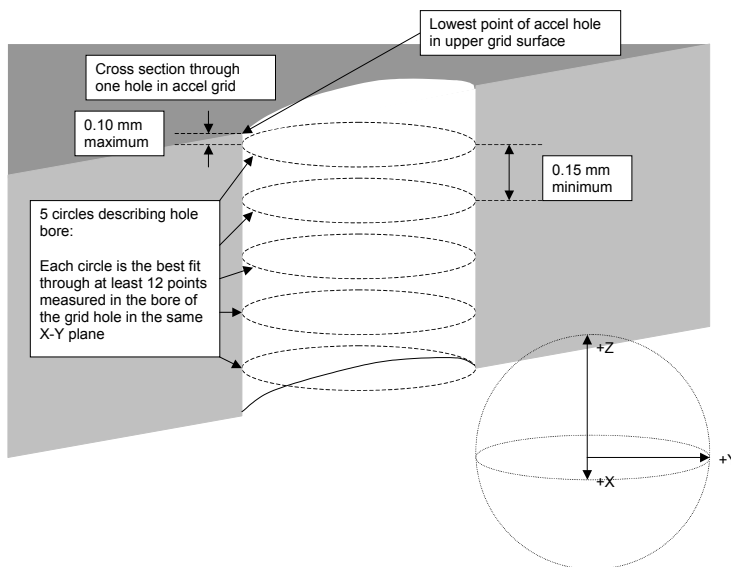


**Figure III-1 Schematic of aperture measurements at different depths in to apertures**

At each depth 12 points were measured equally spaced around the circumference. Software resident in the CMM would then provide the best fit circle to these points along with the circle diameter and the X,Y,Z coordinates of circle centre. These measurements were performed on all of the apertures across the X and Y axes of the grid.

Extrapolation of the aperture erosion is best illustrated by reference to Fig. III-2. The measured diameter increase at each depth was assumed constant and therefore each aperture could be considered as a number of concentric thin cylinders. The diameter increase was then used to calculate a volume increase per cylinder which could then be extrapolated forward.

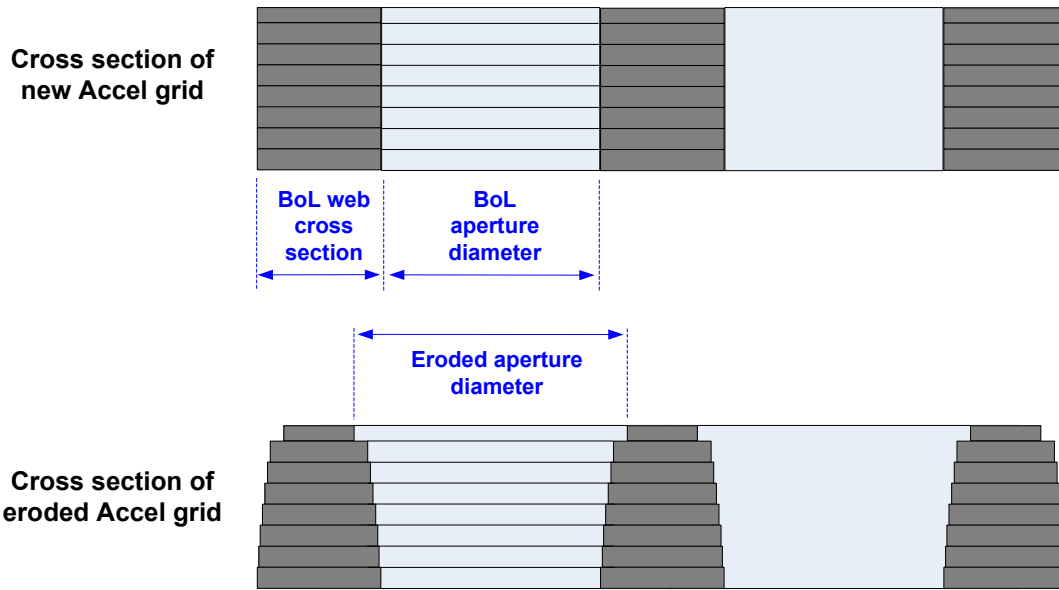


**Figure III-2 Schematic showing division of each aperture into concentric annuluses**

In addition to the aperture measurements the CMM was also used to measure the ‘pits and groove’ erosion on the downstream face. This was achieved by moving the CMM stylus across the webs taking surface measurements at 0.1mm increments between apertures in both the X and Y axes, see Fig. III-3.

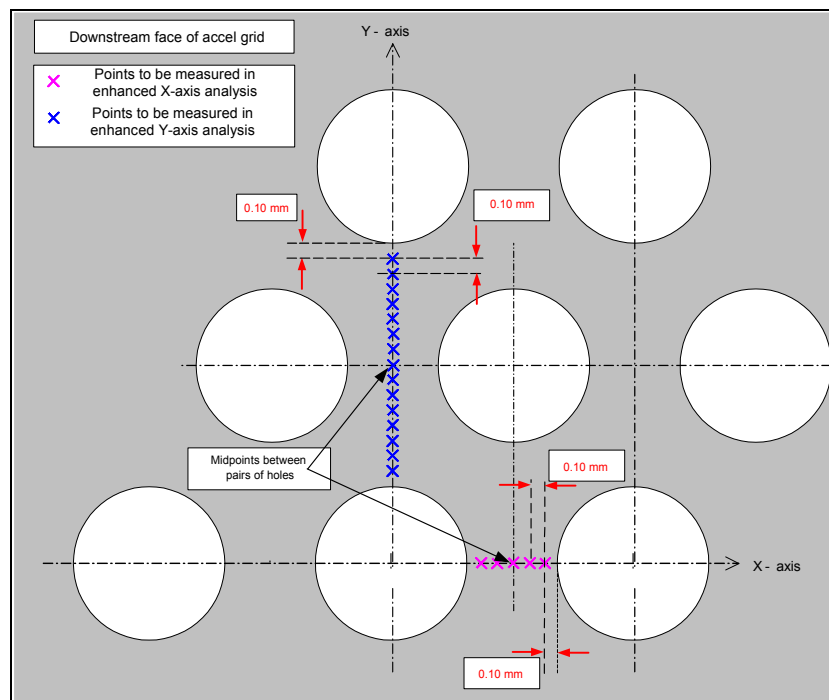


**Figure III-3 Measurement locations between apertures to determine ‘pit and groove’ erosion**

#### IV. Accel grid aperture erosion results

The evolution of the Accel grid apertures is presented in Fig. IV-1, Fig. IV-2 and Fig. IV-3. In these figures the Y-axis is the aperture diameter increase (in mm) w.r.t. the new diameter and the X-axis refers to the aperture number across the grid diameter. The first observation is that the right hand side of the grid (w.r.t. the central aperture) appears to exhibit a different erosion rate than the left hand side. This discrepancy is explained in section A.

A second observation is that effects of the Screen grid optimization become clear after 1820 hours. This manifests itself as a 'saw tooth' change in the aperture diameter increase. This is because there is a step change in the erosion rate between the apertures of differing diameters whereas the steady reduction apparent in each zone is due to the plasma density profile. A third observation is that post 1820hrs the erosion rate in zone 1 appeared to increase significantly. Post 2925hrs however the aperture diameters in zone 1 appear smaller. This is clearly incorrect and is attributed to a measurement error post 1820 hours.

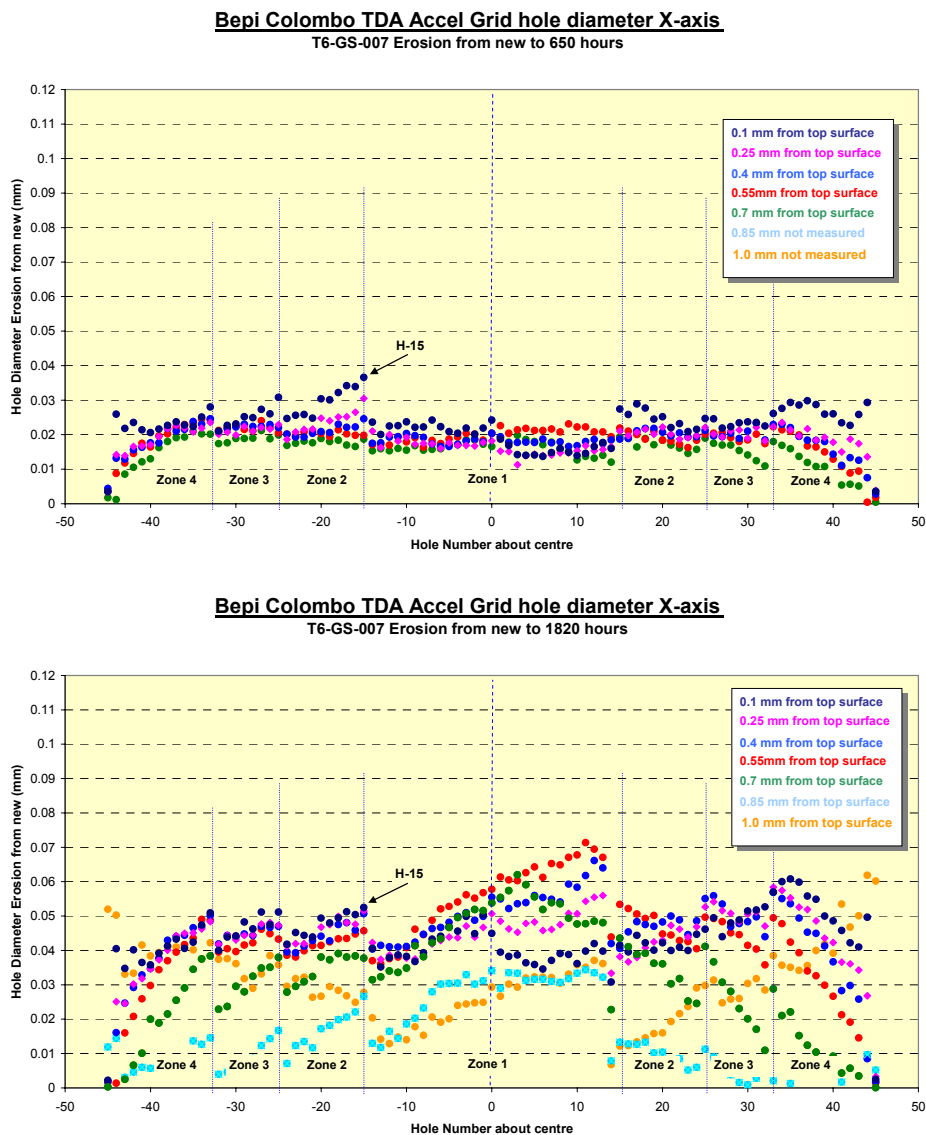
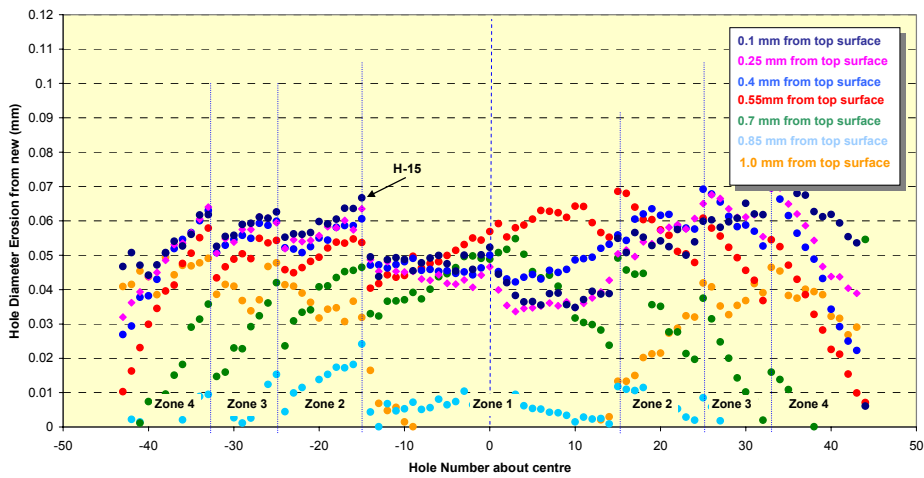
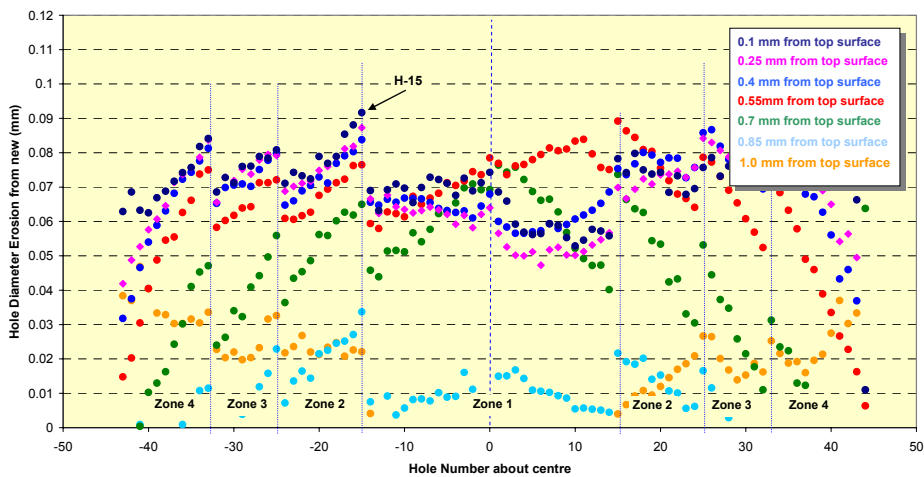


Figure IV-1 Accel aperture diameter increase post 650hrs (top) and 1820hrs (bottom) operation at 175mN

**Bepi Colombo TDA Accel Grid hole diameter X-axis**  
T6-GS-007 Erosion from new to 2925 hours

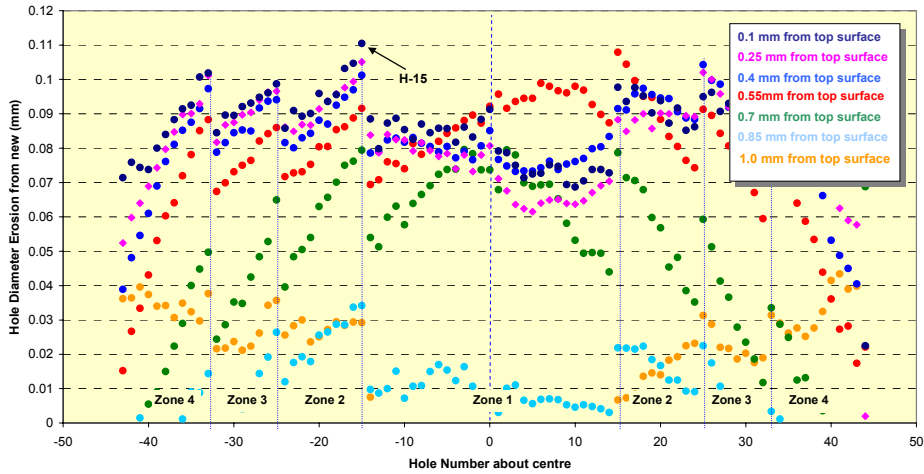


**Bepi Colombo TDA Accel Grid hole diameter X-axis**  
T6-GS-007 Erosion from new to 4040 hours



**Figure IV-2** Accel aperture diameter increase post 2925hrs (top) and 4040hrs (bottom) operation at 175mN

**Bepi Colombo TDA Accel Grid hole diameter X-axis**  
T6-GS-007 Erosion from new to 4840 hours



**Bepi Colombo TDA Accel Grid hole diameter X-axis**  
T6-GS-007 Erosion from new to 6056 hours

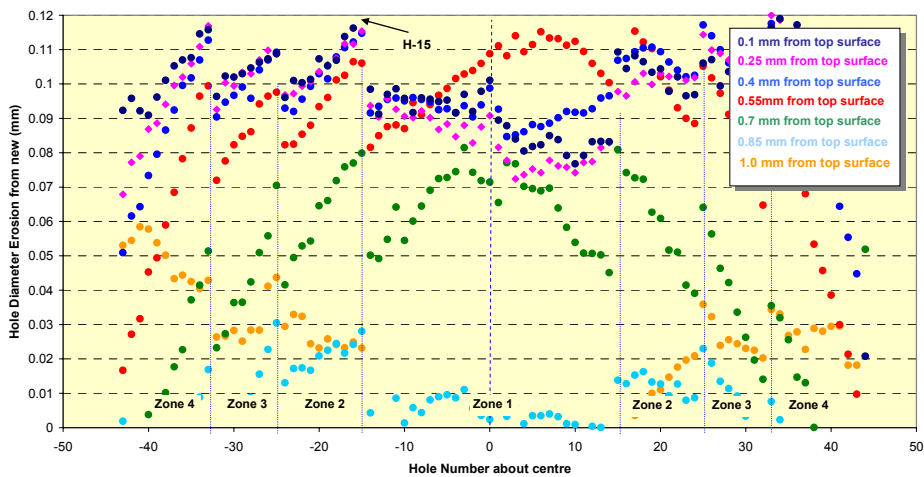


**Figure IV-3 Accel aperture diameter increase post 4840hrs (top) and 6056hrs (bottom) operation at 175mN**

**A. Accel grid manufacture error**

The difference in the erosion of apertures to the right and left of the grid centre can be attributed to a problem that has now been identified in the Accel grid manufacturing process. This resulted in an error in the radial position of the apertures, the magnitude of which depends on its distance from the centre of the grid, see Fig. IV-4.

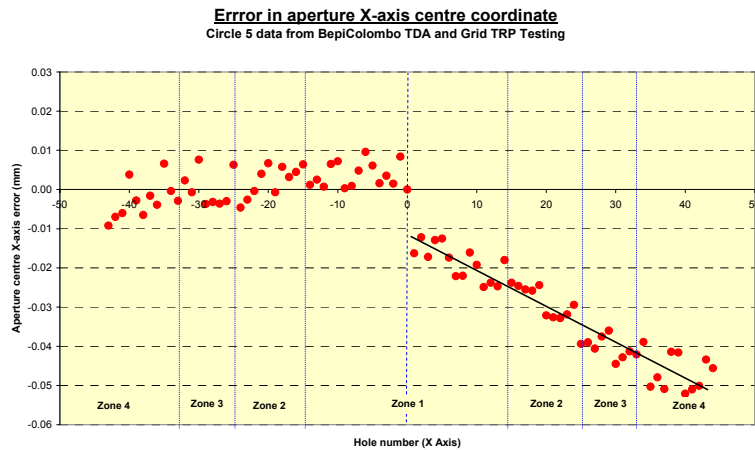


**Figure IV-4 Manufacture error in Accel grid aperture centres**

direction of the asymmetric erosion. This effect is illustrated in Fig. IV-5 which presents the aperture centre movement (Circle 5) w.r.t. the new position as determined at each measurement point. It is clear that the centre of the apertures appear to be moving towards the centre of the Accel grid which is commensurate with the misalignment; i.e. the Accel grid apertures are too close to the grid centre and therefore the asymmetric erosion causes the aperture centre to migrate effectively countering the original error. This also infers that any thrust vector offset resulting from any initial aperture misalignment would slowly reduce, migrating back towards the thruster geometric axis.

As a result the Accel grid apertures are slightly misaligned with those in the screen. This in turn results in asymmetrical CEX erosion on the bore of the aperture and it develops a more elliptical shape, as opposed to a circular shape when aligned.

As described in section III, software resident in the CMM calculates a best fit circle to the 12 points measured around each depth in the apertures and then outputs the diameter and X,Y,Z coordinates of the centre of this circle. Asymmetric aperture erosion therefore manifests itself as slightly larger diameter circles and the centre of the circles appear to migrate in the

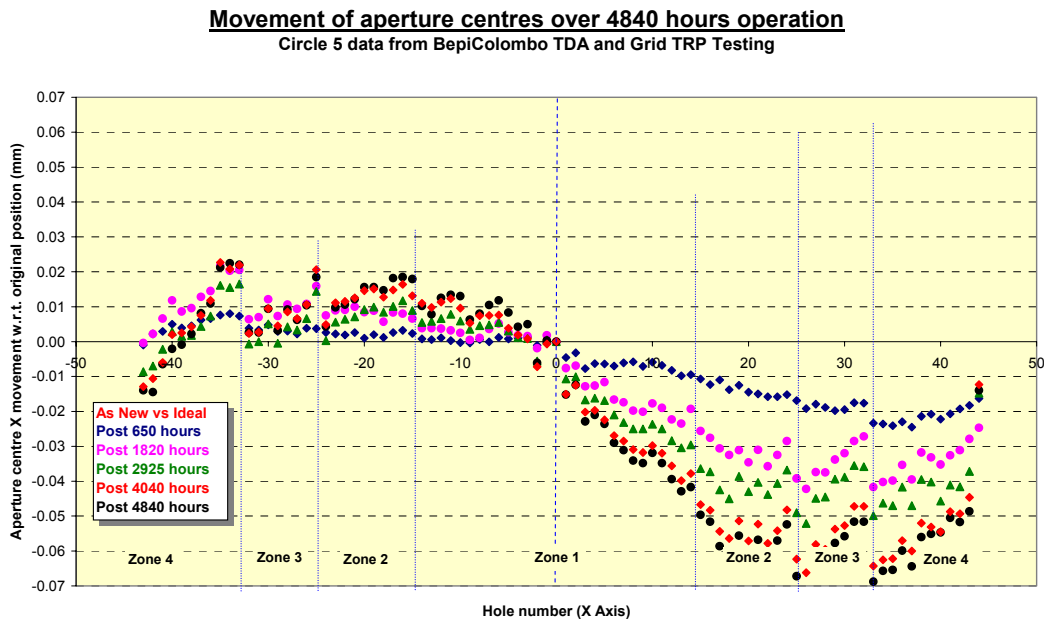


**Figure IV-5 Movement (w.r.t. new position) of apertures across Accel grid X-axis**

The manufacturing error in the Accel grid was caused by the programming of the CNC drilling machine. The grid was drilled in 6 sectors, see Fig. IV-6.

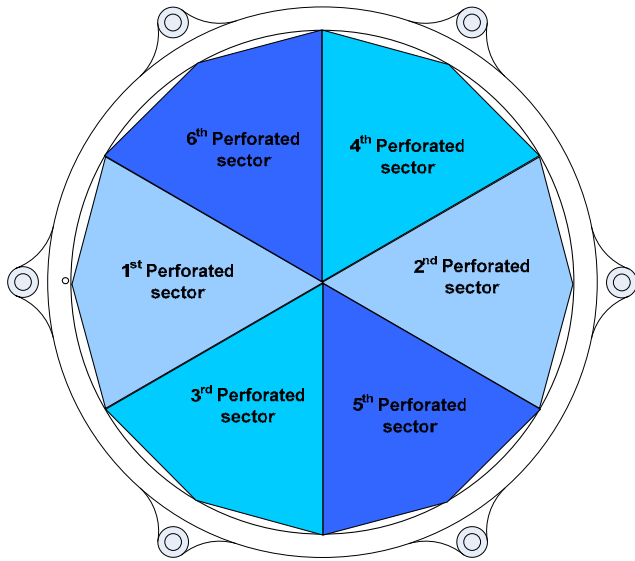


Figure IV-6 Drilling pattern of Accel grid

This approach was adopted because the aperture pattern is symmetric and therefore only a sixth of the apertures needed to be programmed. Once a sector was completed the grid was rotated by 180 degrees and the process repeated.

This approach is perfectly acceptable if the centre of rotation is exactly coincident with the central aperture. If it is not an offset between the apexes of the sectors occurs. This explains the offset shown in Figure IV-4. In addition if the angular rotation is not exactly 180 degrees then the X-axis coordinate of the apertures are smaller than intended and the magnitude of the error increases with increasing distance from the centre.

This problem is readily overcome by programming all apertures and not relying on the rotation of the grid during the drilling process, a modification now implemented on T6.

### B. Extrapolation of Accel aperture erosion

The normalized aperture erosion during the 5 test sequences (measured at 0.1mm, 0.25mm, 0.4mm, 0.55mm and 0.7mm into each aperture) are presented in Fig IV-7 to Fig. IV-11. In these figures the Y-axis is the aperture diameter increase per hour (mm/hour) and the X-axis refers to the aperture number across the grid diameter.

**Bepi Colombo TDA Accel Grid hole diameter X-axis**  
T6-GS-007 Normalised Erosion Rate of Circle 1 (depth 0.1mm)

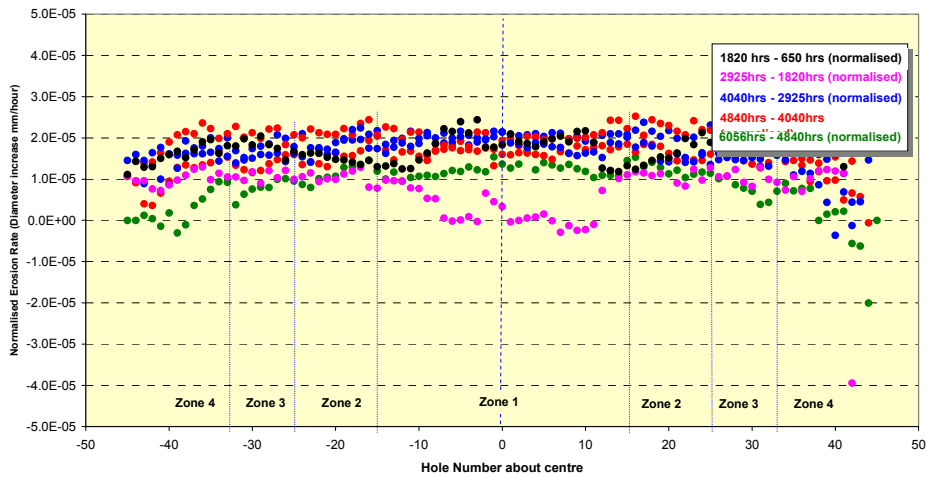
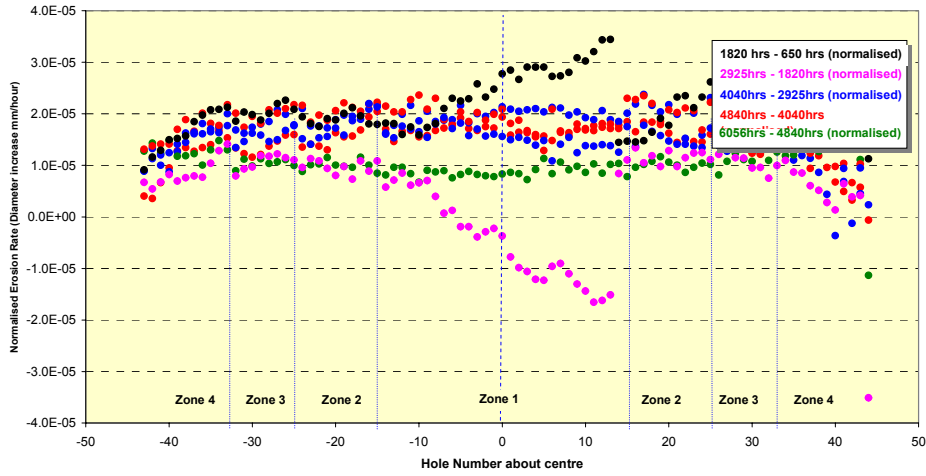


Figure IV-7 Normalized Accel grid erosion rate at 0.1mm depth

**Bepi Colombo TDA Accel Grid hole diameter X-axis**  
T6-GS-007 Normalised Erosion Rate of Circle 2 (depth 0.25mm)



**Figure IV-8 Normalized Accel grid erosion rate at 0.25mm depth**

**Bepi Colombo TDA Accel Grid hole diameter X-axis**  
T6-GS-007 Normalised Erosion Rate of Circle 3 (depth 0.4mm)

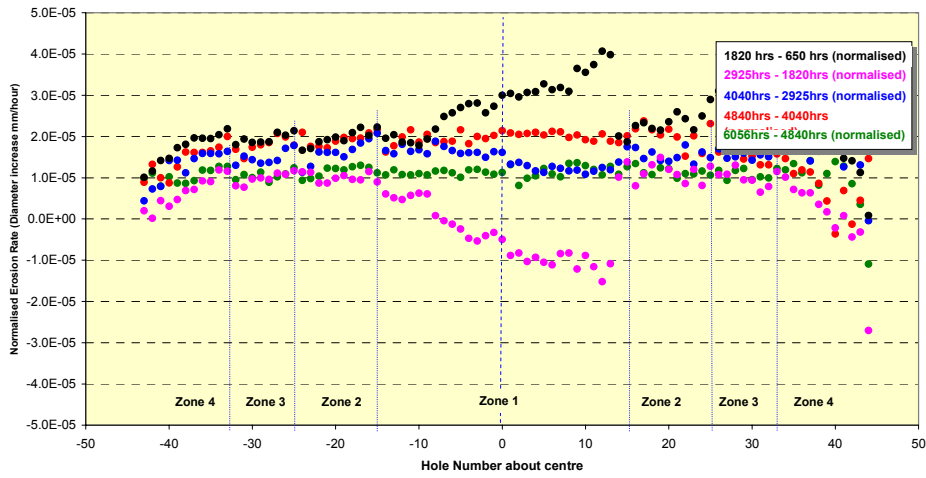


**Figure IV-9 Normalized Accel grid erosion rate at 0.4mm depth**

**Bepi Colombo TDA Accel Grid hole diameter X-axis**  
T6-GS-007 Normalised Erosion Rate of Circle 4 (depth 0.55mm)

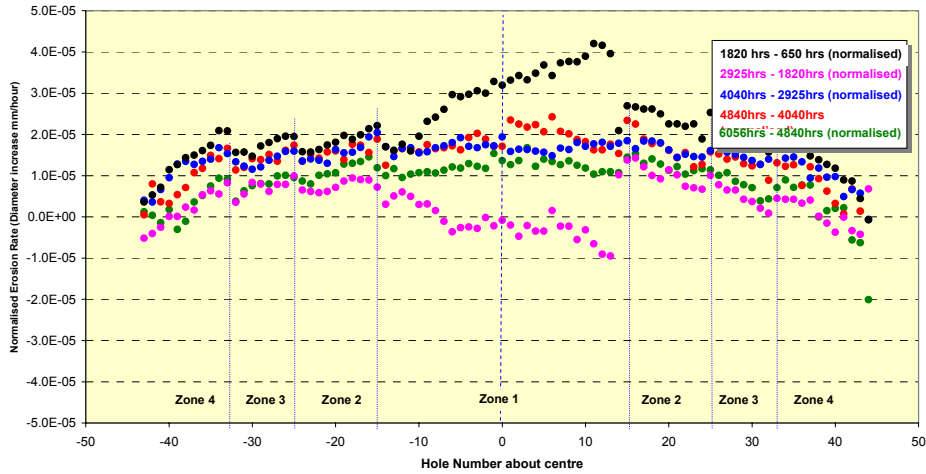


**Figure IV-10 Normalized Accel grid erosion rate at 0.55mm depth**

**Bepi Colombo TDA Accel Grid hole diameter X-axis**  
T6-GS-007 Normalised Erosion Rate of Circle 5 (depth 0.7mm)

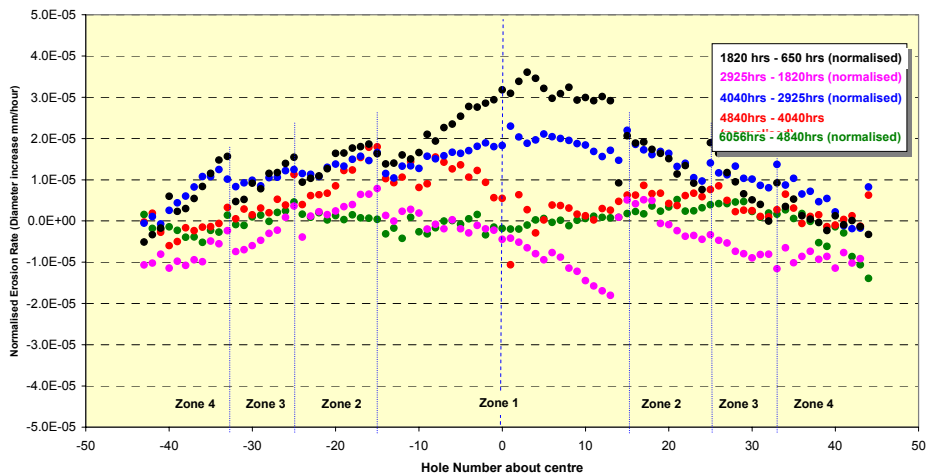


**Figure IV-11 Normalized Accel grid erosion rate at 0.7mm depth**

The spurious nature of the measurements made at 1820hrs is highlighted, particularly in Fig. IV-8. This shows a large increase in apparent erosion at 1820hrs but a subsequent reduction in the apertures diameters at 2925hrs. Ignoring these spurious measurements therefore the worst case aperture erosion occurs at the transition between Zone 1 and Zone 2.

Using the normalized rates at this aperture (H-15) the erosion of this can be extrapolated forward to assess the evolution of this worst case. The result of this analysis is presented in Fig. IV-12. The smallest web thickness

between any two adjacent apertures is 0.85mm and the Accel grid is 1.2mm thick. In Fig. IV-12 the Y-axis is scaled from 0 – 0.85mm, and the X-axis represents the Accel grid thickness of 1.2mm. The plane of the graph can therefore be envisaged as a cross section of the web between two apertures. The web erosion is shown extrapolated to 25MNs.

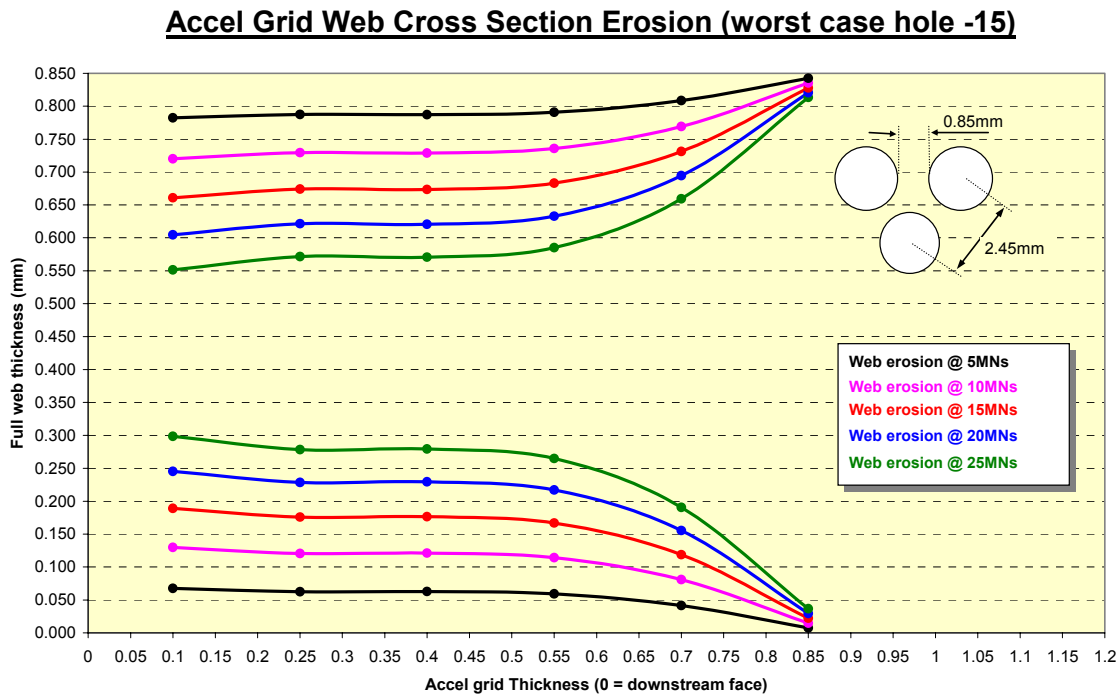


Figure IV-12 Extrapolated worst case web erosion

### V. Accel grid downstream face erosion results

The erosion of the web adjacent to the central aperture is presented in Fig. V-1. It is clear that near the edge of the aperture the web is not being eroded and the peak erosion is apparent in the pits. It should be noted that the stylus employed in the CMM is too large to allow it to reliably measure the bottom of the pits. Depth measurements using an optical non-contact system indicate a maximum pit depth of 0.3 mm as apposed to the maximum of 0.15mm measured using the CMM.

The worst case web groove erosion is 0.033mm, which was accumulated in 5406hrs; i.e. 6056hrs - 650hrs, see Fig. V-1. It was not possible in this case to use the as new grid measurement as the reference because these measurements were made with the Grid prior to fixing to the front pole. Mounting the grid to the front pole imparts a small stress into the grid which causes the grid to slightly deflect in the Z-axis. Unfortunately CMM measurements are not available of the grid (in new condition) following attachment to the front pole.

**Y-Axis Web Surface Erosion (adjacent to central aperture)**

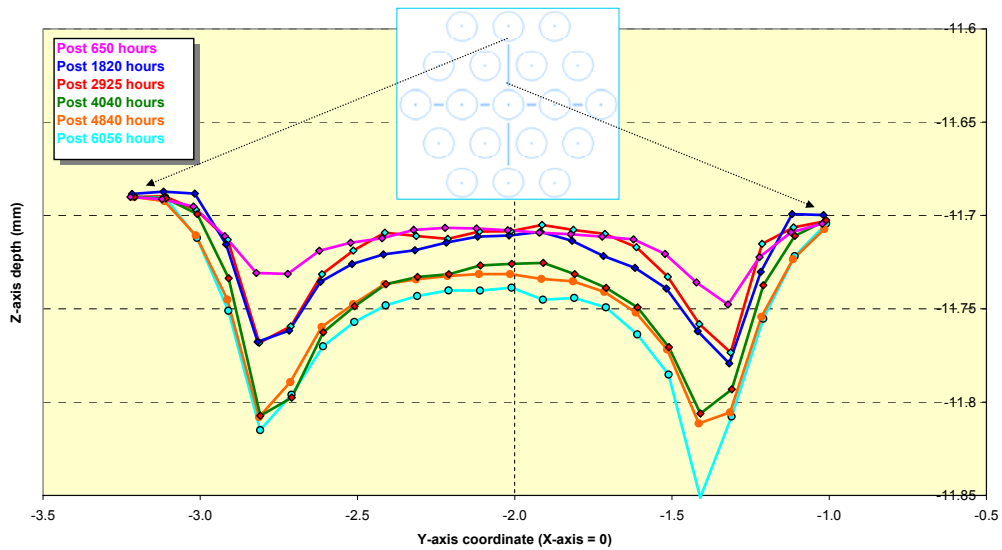


**Figure V-1 Web ‘pit and groove’ erosion on web adjacent to central aperture**

This web erosion is also presented in Fig V-2 where it is drawn to scale and superimposed with a web cross section (shaded area).

**Y-Axis Web Surface Erosion (webs either side of central aperture)**

Drawn to scale to indicate web size w.r.t. erosion pitting

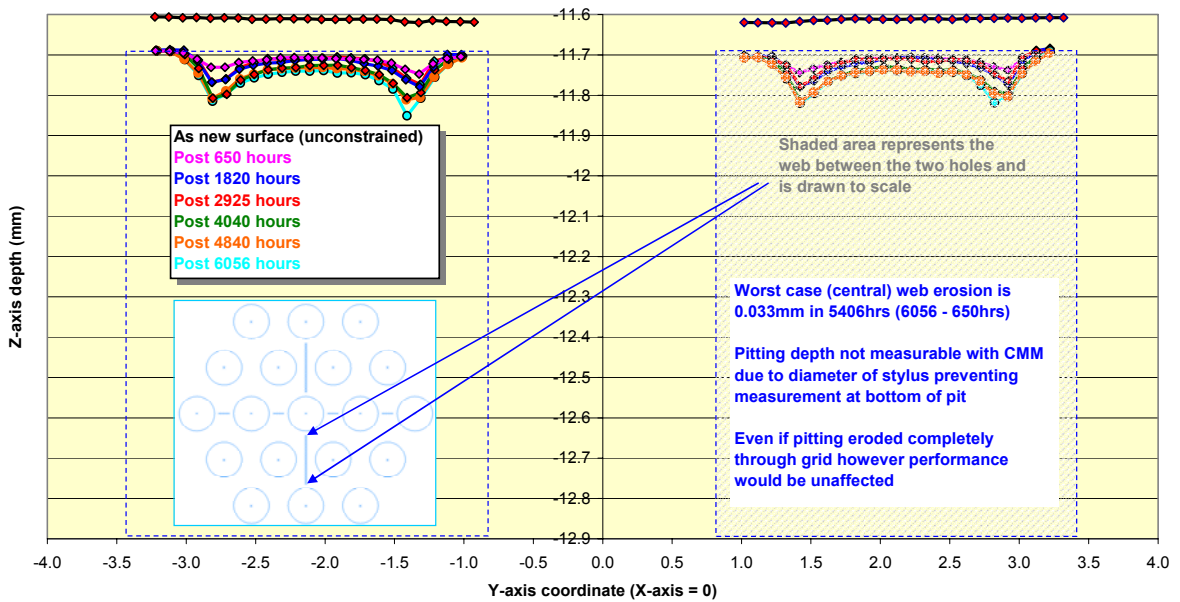


**Figure V-2 Web ‘pit and groove’ erosion either side of the central aperture (drawn to scale)**

Using the worst case erosion of 0.033mm (accumulated in 5406hrs) the effects of the ‘groove’ erosion can also be extrapolated. This extrapolation is presented in Fig V-3 and suggests that the grooves could increase in depth by up to 0.05mm per 5MNs, as compared to a total grid thickness of 1.2 mm.

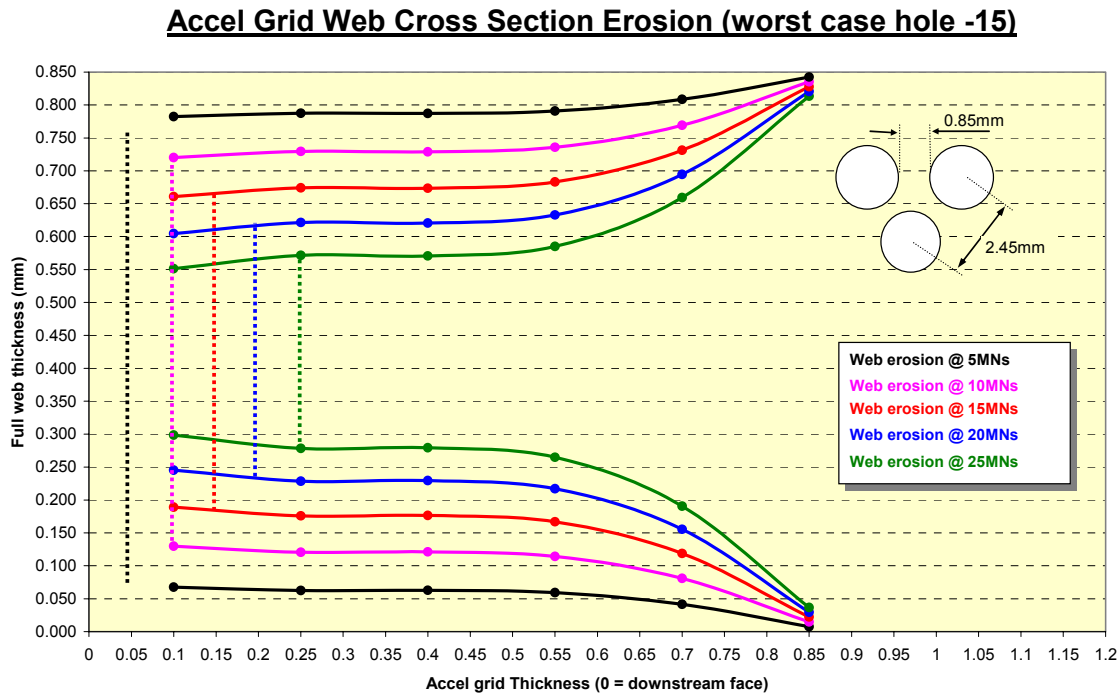


Figure V-3 Extrapolated worst case web erosion including downstream ‘groove’ erosion

## VI. Conclusion

The T6 Accel grid has proved to be extremely resistant to sputter erosion, as demonstrated during the accumulation of  $\sim 3.6 \times 10^6$  Ns and a total operating time of 6056hrs. The T6 grid system was originally optimized to meet the BepiColombo impulse requirement ( $>14 \times 10^6$  Ns) and maximum thrust level ( $>200$  mN) prevalent at the outset of the BepiColombo Phase A studies. During these studies the total impulse requirement has been steadily reduced to  $\sim 10 \times 10^6$  Ns (including a 1.5 qualification margin) and the thrust level has reduced to a maximum of 145 mN. The reduction in the maximum thrust level will result in a further increase in the total impulse capability of the Accel grid and therefore there is an extremely very significant positive margin in the total impulse capability with respect to both the AlphaBus and BepiColombo applications.